

# The Highest Redshift Radio Galaxies

Wil van Breugel<sup>a</sup>

<sup>a</sup>University of California - Lawrence Livermore National Laboratory  
P.O. Box 808, Mailstop L-413, Livermore CA 94551, U.S.A.

## ABSTRACT

At low redshifts powerful radio sources are uniquely associated with massive galaxies, and are thought to be powered by supermassive black holes. Modern 8m – 10m telescopes may be used to find their likely progenitors at very high redshifts to study their formation and evolution.

**Keywords:** High redshift, radio galaxies, massive galaxies, black holes

## 1. WHY THE HIGHEST REDSHIFT RADIO GALAXIES ARE INTERESTING

Within standard Cold Dark Matter scenarios the formation of galaxies is a hierarchical and biased process. Large galaxies are thought to grow through the merging of smaller systems, and the most massive objects form in over-dense regions, which will eventually evolve into the clusters of galaxies seen today (*e.g.* Ref. 1). It has also been suggested that the first massive black holes may grow in similar hierarchical fashion together with their parent galaxies (*e.g.* Ref. 2) or, because of time scale constraints, may precede galaxy formation and be primordial (*e.g.* Ref. 3). It is therefore of great interest to find the progenitors of the most massive galaxies and their AGN (active massive black holes) at the highest possible redshifts and to study their properties and cosmological evolution.

Radio sources are convenient beacons for pinpointing massive elliptical galaxies, at least up to redshifts  $z \sim 1$  (Ref. 4; Ref. 5). The near-infrared ‘Hubble’  $K - z$  relation for such galaxies appears to hold up to  $z = 5.2$ , despite large  $K$ -correction effects and morphological changes (Ref. 6; Fig. 1). This suggests that radio sources may be used to find massive galaxies and their likely progenitors out to very high redshift through near-IR identification.

While optical, ‘color-dropout’ techniques have been successfully used to find large numbers of ‘normal’ young galaxies (without dominant AGN) at redshifts even surpassing those of quasars and radio galaxies (Ref. 7), the radio and near-infrared selection technique has the additional advantage that it is unbiased with respect to the amount of dust extinction. High redshift radio galaxies are therefore also important laboratories for studying the large amounts of dust (*e.g.* Ref. 8) and molecular gas (Ref. 9), which are observed to accompany the formation of the first forming massive galaxies. Indeed, a significant part of the scientific rationale for building future large mm-arrays is based on the expectation that to understand galaxy formation will ultimately require understanding their cold gas and dusty environments.

Finally, it has been claimed that the (co-moving) space densities of the most powerful radio galaxies and quasars were much higher near  $z \sim 2$ , but that they drop off precipitously at even higher redshifts (Ref. 10; Ref. 11). However, using recently completed studies of moderately faint radio galaxies (Ref. 12) it has been argued that here is *no* such evidence for a redshift cut-off and that these previous results have been biased due to unknown radio  $K$ -correction, and thus radio spectral index, trends and associated selection effects.

## 2. HOW TO FIND THE HIGHEST REDSHIFT RADIO GALAXIES

The near-infrared ‘Hubble’  $K - z$  relation for radio galaxies (Fig. 1) provides a convenient tool for finding radio galaxies at ever larger redshifts. This was shown convincingly for the first time by Lilly (Ref. 13) who found that one of the faintest near-IR radio source identifications in a complete, flux limited sample of  $\sim 70$  objects, B3 0924+34, was a redshift  $z = 3.395$ .

Unfortunately in complete, flux-limited samples the vast majority of the sources will be relatively nearby, or at only modest redshifts. Lilly (Ref. 13) in his survey found only 1 / 70 radio galaxies at  $z > 3$ , and McCarthy *et*

---

Further author information: (Send correspondence to W.v.B.)

W.v.B.: E-mail: wil@igpp.llnl.gov

*al.* in a similar but  $\sim 7$  times larger survey also only found one (Ref. 16). However, one can pre-select very good HzRG candidates from the radio catalogs, before even going to the telescope, by choosing sources with ultra-steep radio spectra or ‘red radio color’. It is already known more than 20 years that the identification fraction of radio sources on the POSS plates decreases with increasing spectral index (Ref. 17). One had to wait for the much more sensitive CCD detectors before further progress in identifying ultra-steep spectrum (USS) sources could be made. One of the first HzRGs which was then found, using the Kitt Peak 4m, was the radio galaxy 4C41.17, at  $z = 3.800$  (Ref. 18). This source was the record holder for many years, until it was by-passed, using the same USS method, by 8C 1435+635 ( $z = 4.25$ ; Ref. 19) and 6C 0140+326 ( $z = 4.41$ ; Ref. 20).

Together with graduate student C. De Breuck and colleagues at Leiden Observatory we therefore defined the ‘ultimate’ USS source sample by using several new, large radio surveys (De Breuck *et al.* 2000a [astro-ph/0002297]). The sample consists of 669 sources with extremely steep radio continuum spectra ( $\alpha \leq -1.3$ ; Table 1; Fig. 2), at 10 – 100 times lower flux density limits than has been possible before (Ref. 21; Ref. 22; Ref. 23). To identify these sources we first looked at the POSS and found that approximately  $\sim 15\%$  of the sources could be identified, usually with moderately bright galaxies in galaxy clusters. This identification fraction appears to be independent of spectral index (Fig. 3), at least for  $\alpha \leq -1.3$ , in support of the idea that these are mostly foreground objects.

**Table 1.** USS samples<sup>a</sup>

Sample	Density $\text{sr}^{-1}$	Spectral Index ( $S_\nu \sim \nu^\alpha$ )	Flux Limit mJy	# of Sources
WN	151	$\alpha_{325}^{1400} \leq -1.30$	$S_{1400} > 10$	343
TN	48 <sup>b</sup>	$\alpha_{365}^{1400} \leq -1.30$	$S_{1400} > 10$	268
MP	26	$\alpha_{408}^{4800} \leq -1.20$	$S_{408} > 700$ ; $S_{4850} > 35$	58

<sup>a</sup> See De Breuck *et al.* 2000a (astro-ph/0002297) for catalogs used and other details.

<sup>b</sup> Due to the characteristics of the Texas survey, the TN sample is only  $\sim 30\%$  complete.

The USS selection proved to be extremely efficient. Attempts to obtain optical identifications of USS sources using 3m–4m-class telescopes ( $R \lesssim 24$ ) were largely unsuccessful. Also near-IR imaging would be very difficult, given the typically expected  $R - K \sim 4$  values of high redshift radio galaxies. We therefore decided to entirely skip the optical identification program at Lick Observatory and go straight to near-IR imaging at the Keck I telescope.

### 3. MORPHOLOGICAL EVOLUTION OF THE HIGHEST REDSHIFT RADIO GALAXIES

When we started our near-IR imaging program at Keck our first order of business was to observe high redshift radio galaxies with known redshifts  $z > 1.9$  to investigate their morphological evolution and to obtain more accurate photometry to study the Hubble  $K - z$  diagram at the highest redshifts. We obtained near-IR images of 15 HzRGs with  $1.9 < z < 4.4$  with the Near Infrared Camera (NIRC, Ref. 24) at the Keck I telescope. The images show that there is strong morphological evolution at *rest-frame optical* ( $\lambda_{\text{rest}} > 4000\text{\AA}$ ) wavelengths (Ref. 14; Fig. 4). At the highest redshifts,  $z > 3$ , the rest-frame visual morphologies exhibit structure on at least two different scales: relatively bright, compact components with typical sizes of  $\sim 1''$  ( $\sim 10$  kpc) surrounded by large-scale ( $\sim 50$  kpc) diffuse emission. The brightest components are often aligned with the radio sources, and their *individual* luminosities are  $M_B \sim -20$  to  $-22$ . For comparison, present-epoch  $L_*$  galaxies and, perhaps more appropriately, ultraluminous infrared starburst galaxies, have, on average,  $M_B \sim -21.0$ . The *total, integrated* rest-frame B-band luminosities are 3 – 5 magnitudes more luminous than present epoch  $L_*$  galaxies.

At lower redshifts,  $z < 3$ , the rest-frame optical morphologies become smaller, more centrally concentrated, and less aligned with the radio structure. Galaxy surface brightness profiles for the  $z < 3$  HzRGs are much steeper than those of at  $z > 3$ . We attempted to fit the  $z < 3$  surface brightness profiles with a de Vaucouleurs  $r^{1/4}$  law and with an exponential law, the forms commonly used to fit elliptical and spiral galaxy profiles, respectively. We demonstrate the fitting for our best resolved object at  $z < 3$ , 3C 257 at  $z = 2.474$  (Fig. 4). Within the limited dynamical range of the data, both functional forms fit the observed profiles—neither is preferred. Interestingly, despite this strong

morphological evolution the  $K - z$  Hubble diagram for the most luminous radio galaxies remains valid even at the highest redshifts, where a large fraction of the K-band continuum is due to a radio-aligned component.

Having established that the  $K - z$  diagram for high redshift radio galaxies holds even at the highest known redshifts we embarked on our identification program of USS selected sources. Our typical method of observation would be to begin with 16 x 1 minute exposures (1 minute consisting of 2 or 3 co-added frames), start a second 16 x 1 minute run while reducing the first set of observations using DIMSUM. (DIMSUM is the Deep Infrared Mosaicing Software package, developed by P. Eisenhardt, M. Dickinson, A. Stanford, and J. Ward, which is available as a contributed package in IRAF.) If we could identify our target we would break off our second observation, or, if the identification was faint, would let it finish and then go on to the next target. This ‘on-line’ way of observing turned out to be very efficient and resulted in a 100% identification rate with good photometric magnitudes and has provided excellent high redshift radio galaxy candidates using the Hubble  $K - z$  diagram (Fig. 1; Fig. 5). Often more than a dozen near-IR identifications could be obtained this way in a single night.

#### 4. SPECTROSCOPY OF THE HIGHEST REDSHIFT RADIO GALAXIES

As with our near-IR imaging program, our first spectroscopic observations, using the Low Resolution Imaging Spectrograph (LRIS, Ref. 25) were made of high redshift radio galaxies with known redshifts. The main purpose, initially, was to determine the origin of the radio-aligned optical / near-IR features using spectro-polarimetry. As is now well-known the rest-frame optical continua of high redshift radio galaxies are often clumpy and aligned with their associated radio sources (Ref. 26; Ref. 27). This suggested that there must be a causal connection between their optical morphological appearance and the collimated outflow and/or ionizing radiation from their AGN. The most popular explanations for such an alignment effect are scattered light from hidden or mis-aligned quasars, jet-induced star formation or nebular continuum emission. Evidence for each of these processes has been found. In particular,  $z \sim 1$  and  $z \sim 2.5$  most high redshift radio galaxies are strongly polarized, indicating that a large fraction of the optical continuum is due to scattered light from hidden or mis-aligned quasars (Ref. 28; Ref. 29; Ref. 30). However, deep spectropolarimetry observations of two  $z > 3.5$  radio galaxies (4C 41.17 at  $z = 3.800$  and 6C J1908+722 at  $z = 3.534$ ) show no polarized continua but instead show evidence for absorption lines from young hot stars (Ref. 29). It suggests that at the highest redshifts radio galaxy hosts are dominated by massive starbursts, possibly induced by radio jets (Ref. 31; Ref. 32) and not by scattered light from their AGN.

Subsequently our spectroscopic observations focused on the newly identified USS high redshift radio galaxy candidates. At the present time we have observed and analyzed 34 USS high redshift radio galaxies with the following results. Only 5 of the sources have  $z < 2$ , 8 have  $2 < z < 3$ , 9 have  $3 < z < 4$  and 3 sources have  $z > 4$ , including one at  $z > 5$ . At least 3 sources were not detected in optical continuum, despite  $\sim 1$  hr or longer integrations with LRIS. All we know of these objects is that they are detected in the near-IR at  $K \sim 21$ , and have a radio source identified with them. They may be extremely obscured, or at record high redshifts, with Ly- $\alpha$  redshifted to near-IR wavelengths ( $z > 8$ ). Future observations with near-IR spectrographs may tell. We also found 6 sources with only a continuum detection and no emission-lines. These were all extremely compact USS sources, and may be moderately high redshift ( $1 < z < 3$ ) BL Lac objects, ‘emission-line free quasars’ (*cf.* Ref. 33), or even pulsars (which typically have  $\alpha_{radio} \sim -1.6$ , Ref. 34, and are faint optically).

The high redshift radio galaxy spectra, when obtained with sufficient spectral resolution, show nearly all very strong blueward asymmetries in the Ly- $\alpha$  emission lines (Ref. 29; Ref. 35; De Breuck *et al.* 2000b (in preparation); Fig. 6. This is almost certainly due to the presence of cold gas (HI) and dust in the vicinity of the radio galaxies, not just because of cosmological Ly- $\alpha$  ‘forest’ absorption in the foreground (although this will contribute as well). Spatially resolved emission line regions show that this absorption can occur over the entire region (up to  $\sim 50$  kpc; Fig. 6), and is strongest in the smallest radio sources (Ref. 35). There is much additional evidence for the presence of large amounts of cold gas in dust in high redshift radio galaxies. Many of the highest redshift radio galaxies have been detected at sub-mm wavelengths, both in continuum (*e.g.* Ref. 8; Archibald *et al.* 2000 [astro-ph/0002083]) and molecular lines (*e.g.* Ref. 9). These observations indicate total dust masses of  $10^8 - 10^9 M_{\odot}$ , and star formation rates of more than 1000  $M_{\odot}/\text{yr}$ . Thus high redshift radio galaxies indeed appear to be massive forming systems.

One object deserves special mention: 6C J1908+722 at  $z = 3.53$  (Ref. 29; Fig. 7). The source shows very broad absorption lines in several of its UV resonant lines (CIV, SiIV, NV, Ly- $\alpha$ ; Fig. 8). This was interpreted as being caused by outflow, similar to the classical Broad Absorption Line quasars. However, it is interesting to note that this Broad Absorption Line Radio Galaxy (BALRAG) is hosted by a  $\sim 1.5 \times 10^{13} L_{\odot}$  Ultra Luminous Infrared Galaxy

with  $\sim 1.5 \times 10^8 M_\odot$  in dust,  $\sim 5 \times 10^{10} M_\odot$  in molecular gas, and has an estimated star formation rate of  $\sim 1500 M_\odot/\text{yr}$  (Ref. 9). The observed velocity range of the gas is large ( $530 \text{ km s}^{-1}$ ), and could be even larger: for another high redshift radio galaxy, 4C60.07 at  $z = 3.788$ , Papadopoulos *et al.* find that the molecular gas is distributed over at least two major components, with a total velocity range  $> 1000 \text{ km s}^{-1}$ .

Thus it could very well be that the broad, rest-frame UV, absorption lines in 6C J1908+722 may be due to absorption within the parent galaxy. The large BAL velocity range (Fig. 8) could then be caused by a number of cold gas components in the foreground to 6C J1908+722, and which could be falling in or merging with the galaxy. In that case one would expect that the BAL system would be resolved at higher spectral resolution and observations at Keck to test this are planned.

## 5. THE HIGHEST REDSHIFT RADIO GALAXIES

### 5.1. TN J1338–1942 at $z = 4.11$

The first  $z > 4$  USS radio galaxy discovered by us was TN J1338–1942. The initial identification was made with the ESO 3.6m at R-band, and subsequent spectroscopy with that same telescope showed that the radio galaxy has a redshift of  $z = 4.11 \pm 0.02$ , based on a strong detection of Ly- $\alpha$ , and weak confirming C IV  $\lambda 1549$  and He II  $\lambda 1640$  (Ref. 36).

Subsequently we obtained a deep K-band image (rest-frame B-band) at Keck, shown in Fig. 9 overlaid with a VLA radio image (Ref. 36). The Ly- $\alpha$  and rest-frame optical emission appear co-spatial with the brightest radio hotspot of this very asymmetric radio source. Such asymmetric radio sources are not uncommon, even in the local Universe, and are usually thought to be due to strong interaction of one of its radio lobes with very dense gas. A similar asymmetric radio/optical/emission-line morphology has also been seen in the  $z = 3.800$  radio galaxy 4C41.17, where it has been interpreted as being caused by jet-induced star formation (Ref. 31; Ref. 32; Bicknell *et al.* 2000 [astro-ph/9909218]).

With the Keck K-band the identification and astrometry for TN J1338–1942 secured we next obtained a high signal-to-noise, medium resolution ( $5.5 \text{ \AA}$  FWHM) spectrum using the VLT Antu telescope (Ref. 36; Fig. 10). The spectrum of TN J1338–1942 is dominated by a bright Ly- $\alpha$  line ( $W_{\text{Ly}\alpha}^{\text{rest}} = 210 \text{ \AA}$ ) which shows deep and broad ( $\sim 1400 \text{ km s}^{-1}$ ) blue-ward absorption, and relatively bright ( $F_{1400} \sim 2 \mu\text{Jy}$ ) UV-continuum. In fact, at optical wavelengths, TN J1338–1942 turned out to be the most luminous of its kind (Table 2). If all the UV continuum in TN J1338–1942 would be due to young O–B stars the implied SFR, based on the optical data alone and without correction for extinction, would be several hundred  $M_\odot/\text{yr}$ , similar to 4C41.17. TN J1338–1942 might be another example of a very HzRG in which jet-induced star formation might occur.

The Ly- $\alpha$  is spatially extended by  $\sim 4''$  (30 kpc) and has a spectral profile that is very asymmetric with a deficit towards the blue. This blue-ward asymmetry is probably due to absorption of the Ly- $\alpha$  photons by cold gas in a turbulent halo surrounding the radio galaxy. Using a simple model, and fitting the Ly- $\alpha$  profile with a Gaussian emission function and a single Voigt absorption function, De Breuck *et al.* estimate that the neutral hydrogen column density must be in the range  $3.5 - 13 \times 10^{19} \text{ cm}^{-2}$ , and a total mass of  $2 - 10 \times 10^7 M_\odot$ .

The bright optical continuum and high S/N data also allowed a measurement of the Ly $\alpha$  forest continuum break (Ly- $\alpha$  'discontinuity',  $D_A$ ), and the Lyman limit. The measured value,  $D_A = 0.37 \pm 0.1$ , is  $\sim 0.2$  lower than the values found for quasars at comparable redshifts. This might perhaps be due to a bias towards large  $D_A$  introduced in high-redshift quasar samples that are selected on the basis of large color gradients. The true space density of optically selected quasars, – and Lyman break galaxies –, may have been underestimated and the average HI column density along cosmological lines of sight might have been overestimated. Because of their radio-based, non-color selection,  $z > 4$  radio galaxies may be excellent objects for investigating  $D_A$  statistics.

### 5.2. TN J0924–2201 at $z = 5.19$

TN J0924–2201 is one of the steepest spectrum sources in our USS sample ( $\alpha_{365\text{MHz}}^{1.4\text{GHz}} = -1.63$ ) and therefore was one of our primary targets for near-IR identification. A deep K-band image at Keck showed indeed a very faint ( $K = 21.3 \pm 0.3$ ), multi-component object at the position of the small ( $1.2''$ ) radio source (Fig. 11). The expected redshift on the basis of the  $K - z$  diagram was  $z > 5$ , and spectroscopic observations at Keck showed that this was indeed the case (Fig. 12), based on a single emission line at  $\lambda \sim 7530 \text{ \AA}$  which we identified as Ly- $\alpha$  at  $z = 5.19$  (Ref. 6; none of the  $z > 5$  galaxies have more than one line detection).

**Table 2.** Physical parameters of the highest redshift radio galaxies

Name	$z$	$L_{\text{Ly}\alpha}$ <sup>a</sup>	$L_{365}$ <sup>a</sup>	$\alpha_{365}^{1400}$	$W_{\text{Ly}\alpha}^{\text{rest}}$	$\Delta_{\text{Ly}\alpha}$ <sup>a</sup>	Size <sup>a</sup>	Ref. <sup>b</sup>
TN J0924–2201	5.19	1.3	7.5	−1.63	>115	1500	8	WvB99
VLA J1236+6213	4.42	0.2	0.0035	−0.96	>50	440		Wad99
6C 0140+326	4.41	16	1.3	−1.15	700	1400	19	DeB00
8C 1435+63	4.25	3.2	11	−1.31	670:	1800	28	Spin95
TN J1338–1942	4.11	25	2.3	−1.31	200	1000	37	DeB99
4C 41.17	3.798	12	3.3	−1.25	100	1400	99	Dey97
4C 60.07	3.79	16	4.1	−1.48	150	2900:	65	Röt97

<sup>a</sup> In units of  $10^{43} \text{ erg s}^{-1}$  ( $L_{\text{Ly}\alpha}$ ),  $10^{36} \text{ erg s}^{-1} \text{ Hz}^{-1}$  ( $L_{365}$ ), restframe velocity width  $\text{km s}^{-1}$ , and linear size in kpc (respectively)

<sup>b</sup> Most recent references quoted only: WvB99 = Ref. 6; Wad99 = Ref. 39; DeB00 = De Breuck *et al.* 2000*b* (in preparation); Spin95 = Ref. 40; DeB99 = Ref. 36; Dey97 = Ref. 31; Röt97 = Ref. 37.

Among all radio selected high redshift radio galaxies TN J0924–2201 is fairly typical in radio luminosity, equivalent width and velocity width (Table 2). It does have the steepest radio spectrum, consistent with the  $\alpha - z$  relationship for powerful radio galaxies (*e.g.* Ref. 37), and also has the smallest linear size. The latter may be evidence of its ‘inevitable youthfulness’ or a dense confining environment, neither of which would be surprising because of its extreme redshift (Ref. 38; Ref. 35). Among the radio selected high redshift radio galaxies TN J0924–2201 appears underluminous in  $\text{Ly-}\alpha$ , together with 8C 1435+63, which might be caused by absorption in an exceptionally dense cold and dusty medium. Evidence for cold gas and dust in several of the most distant high redshift radio galaxies has been found from sub-mm continuum and CO-line observations (*e.g.* Ref. 8; Ref. 9).

The second highest redshift radio galaxy currently known listed in Table 2 is VLA J123642+621331 at  $z = 4.42$  (Ref. 39). This source was not USS selected and provides a view on the possible selection effects of our USS high redshift radio galaxies. The source is an asymmetric double and although its radio luminosity is about a factor 1000 times lower than that of its much more luminous brothers at similar redshifts, it is still radio loud, with a radio luminosity close to the FRI / FRII break at 408 MHz ( $P_{408} \sim 3.2 \times 10^{33} \text{ erg s}^{-1} \text{ Hz}^{-1}$ ). Its radio spectrum is steep ( $\alpha_{8.4\text{GHz}}^{1.4\text{GHz}} \sim -1.0$ , using the flux densities given by Waddington *et al.*), but not as steep as our USS selected high redshift radio galaxies, and the  $\text{Ly-}\alpha$  luminosity is a factor 5 – 10 times less. Apart from the luminosity these properties are not hugely different from expected on the basis of radio selection. It suggests that less extreme steep spectrum selected samples ( $\alpha < -1.0$ ) at much lower flux densities ( $\lesssim 1 \text{ mJy}$ ) might be used to find many more high redshift radio galaxies at very high redshifts, although with lower efficiency, we suspect, than USS selected samples.

Our observations of TN J0924–2201 extend the Hubble  $K - z$  diagram for powerful radio galaxies to  $z = 5.19$ , as shown in Fig. 1. Simple stellar evolution models are shown for comparison. Despite the enormous  $k$ -correction effect (from  $U_{\text{rest}}$  at  $z = 5.19$  to  $K_{\text{rest}}$  at  $z = 0$ ) and strong morphological evolution (from radio-aligned to elliptical structures), the  $K - z$  diagram remains a powerful phenomenological tool for finding radio galaxies at extremely high redshifts. Deviations from the  $K - z$  relationship may exist (Ref. 15; but see Ref. 41), and scatter in the  $K - z$  values appears to increase with redshift. Part of this may be due to lack of S/N or contamination by strong line emission in some of the measurements.

The clumpy  $U_{\text{rest}}$  morphology resembles that of other high redshift radio galaxies (Ref. 32; Ref. 42) and if it is dominated by star light we derive a SFR of  $\sim 200 \text{ M}_{\odot} \text{ yr}^{-1}$ , without any correction for extinction, which may be a factor of several. TN J0924–2201 may be a massive, active galaxy in its formative stage, in which the SFR is boosted by jet-induced star formation. For comparison other, ‘normal’ star forming galaxies at  $z > 5$  have 10 – 30 times lower SFR ( $\sim 6 - 20 \text{ M}_{\odot}/\text{yr}$ ).

At the time of its discovery, December 1998, TN J0924–2201 was the most distant AGN known, surpassing even quasars for the first time since their discovery 36 years ago. The recent, serendipitous discovery of a color-selected  $z = 5.50$  quasar (Stern *et al.* 2000 [astro-ph/0002338]) returned the record to optically selected quasars. The presence of AGN at such early epochs in the Universe ( $< 1 \text{ Gyr}$  in most cosmogonies) poses interesting challenges to common theoretical wisdom, which assumes, at least for radio loud AGN, that they are powered by massive (billion solar

mass), active black holes. The question how these can form so shortly after the putative Big Bang may prove even more challenging than that of the formation of galaxies (*e.g.* Ref. 3).

## ACKNOWLEDGMENTS

WvB thanks his many collaborators for stimulating discussions and fun observing runs. Special thanks to C. De Breuck, who has done much of the work as part of his thesis research, and A. Dey for permission to use Fig. 6, Fig. 7 and Fig. 8. The work by W.v.B. at the University of California Lawrence Livermore National Laboratory was performed under the auspices of the US Department of Energy under contract W-7405-ENG-48. W.v.B. also acknowledges support from several NASA grants in support of high redshift radio galaxy research with HST.

## REFERENCES

1. S. D. M. White, "The physical origin of galaxy scaling relations," in *Galaxy Scaling Relations: Origins, Evolution and Applications*, pp. 3+, 1997.
2. G. Kauffmann and M. Haehnelt, "A unified model for the evolution of galaxies and quasars," *MNRAS* **311**, pp. 576–588, jan 2000.
3. A. Loeb, "Cosmological formation of quasar black holes," *ApJ* **403**, pp. 542–551, feb 1993.
4. S. J. Lilly and M. S. Longair, "Stellar populations in distant radio galaxies," *MNRAS* **211**, pp. 833–855, dec 1984.
5. P. N. Best, M. S. Longair, and H. J. A. Rottgering, "Hst, radio and infrared observations of 28 3cr radio galaxies at redshift  $z$  approximately equal to 1. ii - old stellar populations in central cluster galaxies," *MNRAS* **295**, pp. 549+, apr 1998.
6. W. J. M. van Breugel, C. D. Breuck, S. A. Stanford, D. Stern, H. J. A. Rottgering, and G. K. Miley, "A radio galaxy at  $z = 5.19$ ," *ApJL* **518**, pp. L61–L64, jun 1999.
7. R. J. Weymann, D. Stern, A. Bunker, H. Spinrad, F. H. Chaffee, R. I. Thompson, and L. J. Storrie-Lombardi, "Keck spectroscopy and nicmos photometry of a redshift  $z = 5.60$  galaxy," *ApJ* **505**, pp. L95–L98, oct 1998.
8. R. J. Ivison, J. S. Dunlop, D. H. Hughes, E. N. Archibald, J. A. Stevens, W. S. Holland, E. I. Robson, S. A. Eales, S. Rawlings, A. Dey, and W. K. Gear, "Dust, gas, and evolutionary status of the radio galaxy 8c 1435+635 at  $z = 4.25$ ," *ApJ* **494**, pp. 211+, feb 1998.
9. P. P. Papadopoulos, H. J. A. Rottgering, P. P. van Der Werf, S. Guilloteau, A. Omont, W. J. M. van Breugel, and R. P. J. Tilanus, "Co (4-3) and dust emission in two powerful high- $z$  radio galaxies, and co lines at high redshifts," *ApJ* **528**, pp. 626–636, jan 2000.
10. J. S. Dunlop and J. A. Peacock, "The redshift cut-off in the luminosity function of radio galaxies and quasars," *MNRAS* **247**, pp. 19+, nov 1990.
11. P. A. Shaver, J. V. Wall, K. I. Kellermann, C. A. Jackson, and M. R. S. Hawkins, "Decrease in the space density of quasars at high redshift," *Nature* **384**, pp. 439–441, 1996.
12. M. J. Jarvis, S. Rawlings, C. J. Willott, K. M. Blundell, S. Eales, and M. Lacy, "No evidence for a 'redshift-cut-off' for the most powerful classical double radio sources," in *The Hy-Redshift Universe: Galaxy Formation and Evolution at High Redshift*, A. J. Bunker and W. J. M. van Breugel, eds., *ASP Conf. Series* **193**, pp. 90+, 1999.
13. S. J. Lilly, "Discovery of a radio galaxy at a redshift of 3.395," *ApJ* **333**, pp. 161–167, oct 1988.
14. W. J. M. van Breugel, S. A. Stanford, H. Spinrad, D. Stern, and J. R. Graham, "Morphological evolution in high-redshift radio galaxies and the formation of giant elliptical galaxies," *ApJ* **502**, pp. 614+, aug 1998.
15. S. Eales, S. Rawlings, D. Law-Green, G. Gotter, and M. Lacy, "A first sample of faint radio sources with virtually complete redshifts. i - infrared images, the hubble diagram and the alignment effect," *MNRAS* **291**, pp. 593+, nov 1997.
16. P. J. McCarthy, V. K. Kapahi, W. J. M. van Breugel, S. E. Persson, R. Athreya, and C. R. Subrahmanya, "The molonglo reference catalog/1 jansky radio source survey. i. radio galaxy identifications," *ApJS* **107**, pp. 19+, nov 1996.
17. A. G. G. M. Tielens, G. K. Miley, and A. G. Willis, "Westerbork observations of 4c sources with steep radio spectra," *A&ASup* **35**, pp. 153+, feb 1979.
18. K. C. Chambers, G. K. Miley, and W. J. M. van Breugel, "4c 41.17 - a radio galaxy at a redshift of 3.8," *ApJ* **363**, pp. 21–39, nov 1990.

19. M. Lacy, G. Miley, and S. R. et. al., "8c 1435+635: a radio galaxy at  $z=4.25$ ," *MNRAS* **271**, pp. 504–512, nov 1994.
20. S. Rawlings, M. Lacy, K. M. Blundell, S. A. Eales, A. J. Bunker, and S. T. Garrington, "A radio galaxy at redshift 4.41," *Nature* **383**, pp. 502–505, 1996.
21. K. C. Chambers, G. K. Miley, W. J. M. van Breugel, and J. S. Huang, "Ultra-steep-spectrum radio sources. i. 4c objects," *ApJS* **106**, pp. 215+, oct 1996.
22. H. J. A. Rottgering, M. Lacy, G. K. Miley, K. C. Chambers, and R. Saunders, "Samples of ultra-steep spectrum radio sources," *A&ASup* **108**, pp. 79–141, nov 1994.
23. K. M. Blundell, S. Rawlings, S. A. Eales, G. B. Taylor, and A. D. Bradley, "A sample of 6c radio sources designed to find objects at redshift  $z > 4$  - i. the radio data," *MNRAS* **295**, pp. 265–279, apr 1998.
24. K. Matthews and B. T. Soifer, "The near infrared camera on the w. m. keck telescope," *Experimental Astronomy* **3**, pp. 77–84, 1994.
25. J. B. Oke, J. G. Cohen, M. Carr, J. Cromer, A. Dingizian, F. H. Harris, S. Labrecque, R. Lucinio, W. Schaal, H. Epps, and J. Miller, "The keck low-resolution imaging spectrometer," *PASP* **107**, pp. 375+, apr 1995.
26. P. J. McCarthy, W. J. M. van Breugel, H. Spinrad, and S. Djorgovski, "A correlation between the radio and optical morphologies of distant 3cr radio galaxies," *ApJL* **321**, pp. L29–L33, oct 1987.
27. K. C. Chambers, G. K. Miley, and W. J. M. van Breugel, "Alignment of radio and optical orientations in high-redshift radio galaxies," *Nature* **329**, pp. 604–606, oct 1987.
28. A. Cimatti, S. di Serego Alighieri, J. Vernet, M. H. Cohen, and R. A. E. Fosbury, "No signs of starbursts in  $z \sim 2.5$  radio galaxies," in *The Most Distant Radio Galaxies*, H. J. A. Rottgering, P. N. Best, and M. D. Lehnert, eds., *KNAW Colloq* **49**, pp. 195+, 1999.
29. A. Dey, "The early history of powerful radio galaxies," in *The Most Distant Radio Galaxies*, H. J. A. Rottgering, P. N. Best, and M. D. Lehnert, eds., *KNAW Colloq* **49**, pp. 19+, 1999.
30. J. Vernet, R. A. E. Fosbury, M. Villar-Martin, M. H. Cohen, S. di Serego Alighieri, and A. Cimatti, "Keck spectropolarimetry of  $\sim 2.5$  radio galaxies," in *The Hy-Redshift Universe: Galaxy Formation and Evolution at High Redshift*, A. J. Bunker and W. J. M. van Breugel, eds., *ASP Conf. Series* **193**, pp. 102+, 1999.
31. A. Dey, W. J. M. van Breugel, W. D. Vacca, and R. Antonucci, "Triggered star formation in a massive galaxy at  $z = 3.8$ : 4c 41.17," *ApJ* **490**, pp. 698+, dec 1997.
32. W. J. M. van Breugel, A. S. Stanford, and A. D. et. al., "Induced star formation and morphological evolution in very high redshift radio galaxies," in *The Most Distant Radio Galaxies*, H. J. A. Rottgering, P. N. Best, and M. D. Lehnert, eds., *KNAW Colloq* **49**, pp. 49+, 1999.
33. X. Fan, M. A. Strauss, and J. E. G. et. al., "The discovery of a high-redshift quasar without emission lines from sloan digital sky survey commissioning data," *ApJL* **526**, pp. L57–L60, dec 1999.
34. D. L. Kaplan, J. J. Condon, Z. Arzoumanian, and J. M. Cordes, "Pulsars in the nrao vla sky survey," *ApJS* **119**, pp. 75–82, nov 1998.
35. R. van Ojik, H. J. A. Rottgering, G. K. Miley, and R. W. Hunstead, "The gaseous environments of radio galaxies in the early universe: kinematics of the lyman- $\alpha$  emission and spatially resolved h i absorption," *A&A* **317**, pp. 358–384, jan 1997.
36. C. D. Breuck, W. J. M. van Breugel, D. Minniti, G. K. Miley, H. Rottgering, S. A. Stanford, and C. Carilli, "Vlt spectroscopy of the  $z=4.11$  radio galaxy tn j1338–1942," *A&A* **352**, pp. L51–L56, dec 1999.
37. H. J. A. Rottgering, R. van Ojik, G. K. Miley, K. C. Chambers, W. J. M. van Breugel, and S. de Koff, "Spectroscopy of ultra-steep spectrum radio sources: a sample of  $z > 2$  radio galaxies," *A&A* **326**, pp. 505–527, oct 1997.
38. K. M. Blundell and S. Rawlings, "The inevitable youthfulness of known high-redshift radio galaxies," *Nature* **399**, pp. 330–332, may 1999.
39. I. Waddington, R. A. Windhorst, S. H. Cohen, R. B. Partridge, H. Spinrad, and D. Stern, "Nicmos imaging of the dusty microjansky radio source vla j123642+621331 at  $z = 4.424$ ," *ApJL* **526**, pp. L77–L80, dec 1999.
40. H. Spinrad, A. Dey, and J. R. Graham, "Keck observations of the most distant galaxy: 8c 1435+63 at  $z = 4.25$ ," *ApJL* **438**, pp. L51–L54, jan 1995.
41. P. McCarthy, "Recent results from the mrc/1jy survey," in *The Most Distant Radio Galaxies*, H. J. A. Rottgering, P. N. Best, and M. D. Lehnert, eds., *KNAW Colloq* **49**, pp. 5+, 1999.
42. L. Pentericci, H. J. A. Rottgering, and G. K. M. et. al., "Hst images of the extremely clumpy radio galaxy 1138-262 at  $z = 2.2$ ," *ApJ* **504**, pp. 139+, sep 1998.

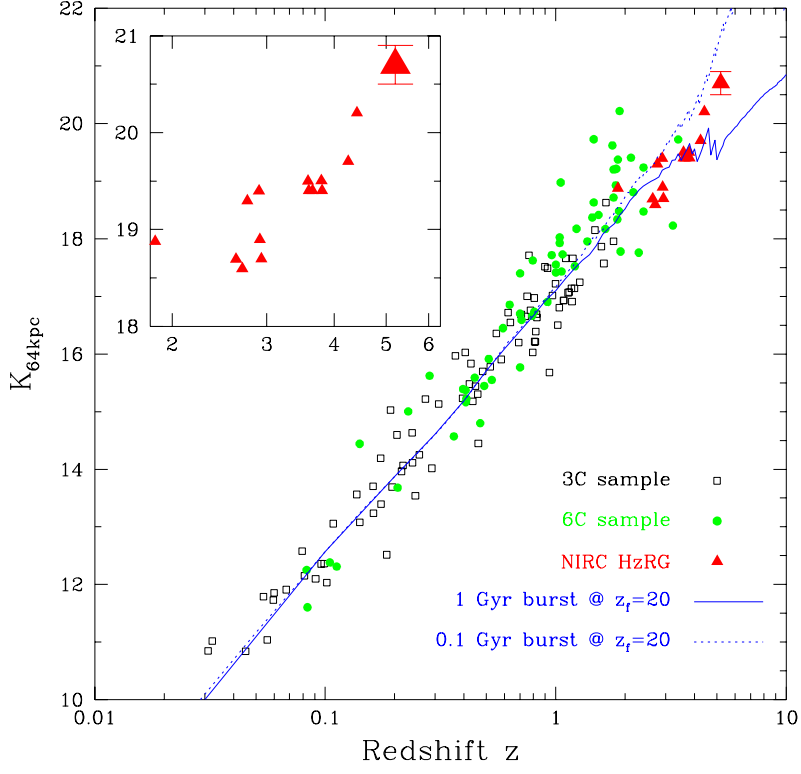


**Figure 1.** The Hubble  $K - z$  diagram for high redshift radio galaxies. Filled triangles are Keck measurements of high redshift radio galaxies from Ref. 14, the large triangle is TN J0924-2201 at  $z = 5.19$ , and all other photometry is from Ref. 15. Two stellar evolution models from Bruzual and Charlot (1999; priv. comm.) normalized at  $z < 0.1$ , are plotted, assuming parameters as shown.



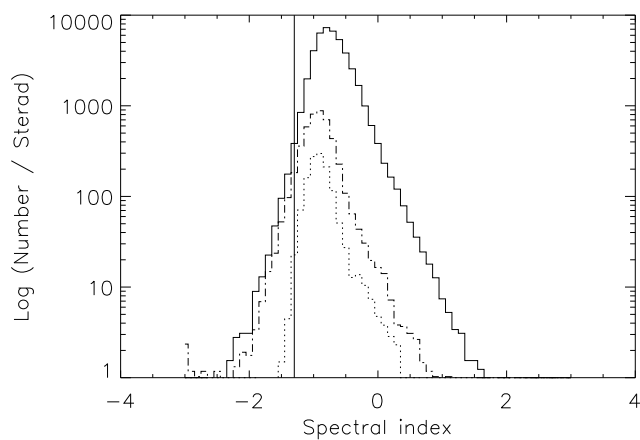


**Figure 2.** Logarithmic spectral index distribution for WENSS-NVSS (full line), Texas-NVSS (dot-dash line) and MRC-PMN (dotted line). The vertical line indicates the  $-1.3$  cutoff used in our spectral index selection.

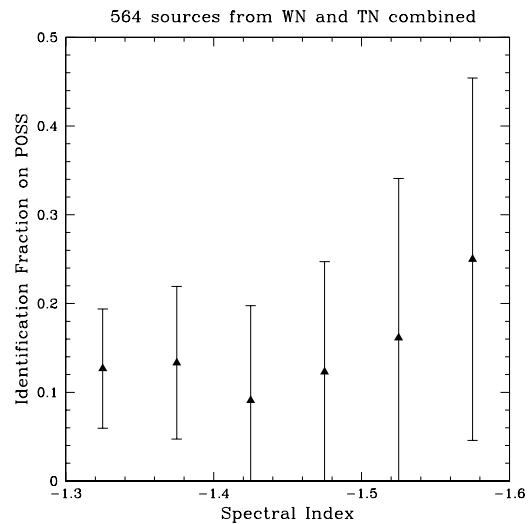


**Figure 3.** Identification fraction on the POSS as a function of spectral index for the combined WN and TN sample.

This figure is available as fig4.jpg

**Figure 4.** Selected near-IR images of high redshift radio galaxies, presented in order of decreasing redshift, and the surface brightness profile of 3C257.

This figure is available as fig5.jpg

**Figure 5.** Some of our faintest Keck near-IR identifications of USS sources. Typical exposures with NIRC were  $\sim 1$  hr. Spectroscopy of one the faintest objects, TN J0924–2201 , showed it to be at  $z = 5.19$  (Section 5.2).

This figure is available as fig6.jpg

**Figure 6.** Ly-alpha emission profiles of four high redshift radio galaxies (Figure and caption from Ref. 29). The triangular-shaped profiles result from spatially extended absorption which is blue-shifted relative to the systemic velocity. The zero velocity in all cases is determined either from the HeII $\lambda$ 1640 line or the CIII] $\lambda$ 1909 line. Note that the Ly- $\alpha$  emission from 4C41.17 extends over  $> 200$  kpc.

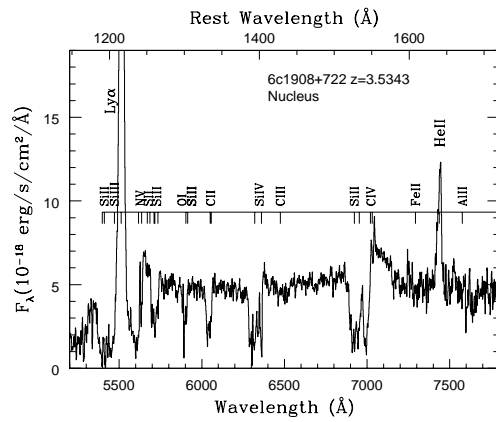


**Figure 7.** Spectrum of the  $z = 3.53$  BALRAG 6C 1908+722 (Figure from Ref. 29).

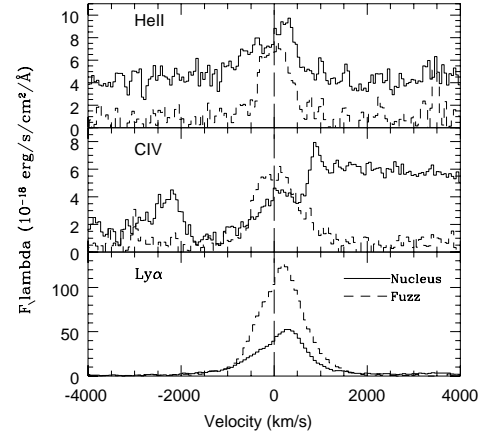


**Figure 8.** The  $\text{Ly}\alpha$ , CIV and HeII line profiles. Note that the profiles appear to be asymmetric both on and off the nucleus (Figure from Ref. 29).

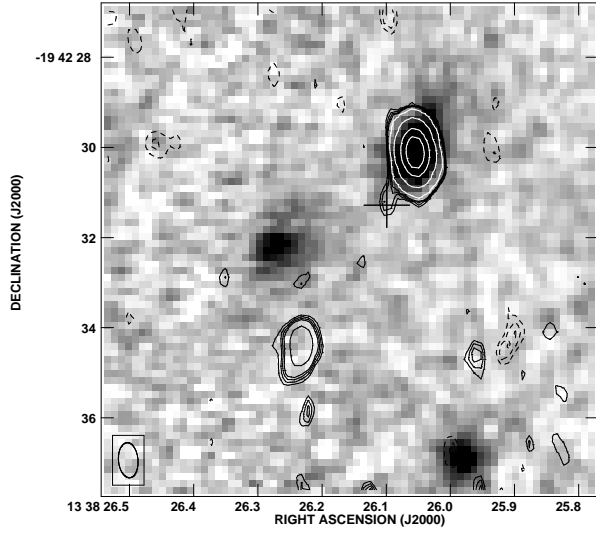


**Figure 9.** 4.85 GHz VLA radio contours overlaid on a Keck *K*-band image of TN J1338–1942 .

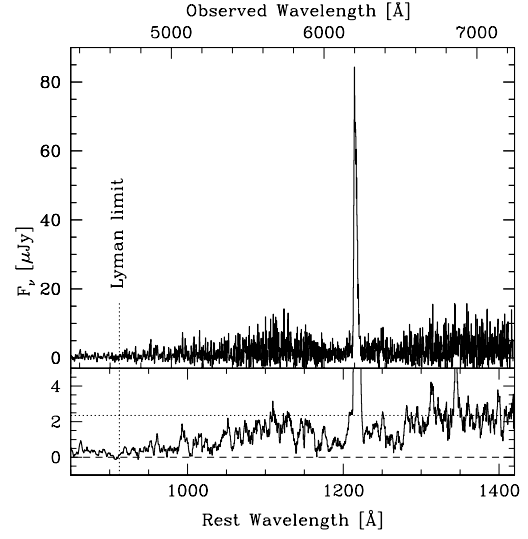


**Figure 10.** VLT spectrum of TN J1338–1942 at  $z = 4.11$ .

This figure is available as fig11.jpg

**Figure 11.** Keck/NIRC *K*-band image of TN J0924–2201 , with radio contours superposed.

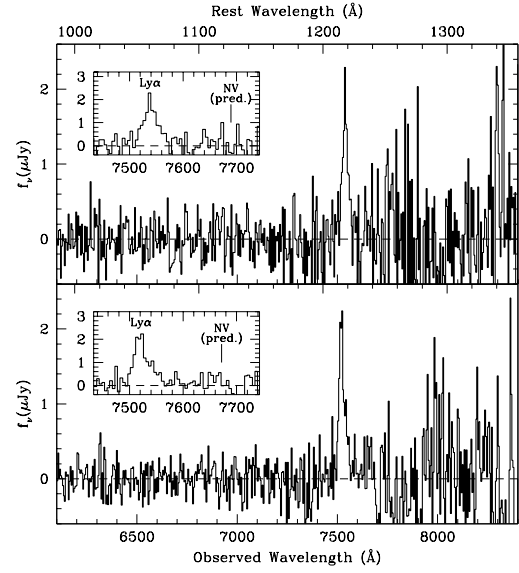


**Figure 12.** Keck spectra of TN J0924–2201 at  $z = 5.19$  on two different nights.

This figure "fig4.jpg" is available in "jpg" format from:

<http://arxiv.org/ps/astro-ph/0006238v1>



This figure "fig5.jpg" is available in "jpg" format from:

<http://arxiv.org/ps/astro-ph/0006238v1>

This figure "fig6.jpg" is available in "jpg" format from:

<http://arxiv.org/ps/astro-ph/0006238v1>

This figure "fig11.jpg" is available in "jpg" format from:

<http://arxiv.org/ps/astro-ph/0006238v1>